

# Solid olive waste in environmental cleanup: Oil recovery and carbon production for water purification

Amer El-Hamouz<sup>a</sup>, Hikmat S. Hilal<sup>b,\*</sup>, Nashaat Nassar<sup>a</sup>, Zahi Mardawi<sup>a</sup>

<sup>a</sup>Department of Chemical Engineering, An-Najah National University, P.O. Box 7, Nablus, Palestine

<sup>b</sup>Department of Chemistry, An-Najah National University, P.O. Box 7, Nablus, Palestine

Received 3 September 2005; received in revised form 12 May 2006; accepted 17 May 2006

Available online 10 July 2006

## Abstract

A potentially-economic three-fold strategy, to use solid olive wastes in water purification, is presented. Firstly, oil remaining in solid waste (higher than 5% of waste) was recovered by the Soxhlet extraction technique, which can be useful for the soap industry. Secondly, the remaining solid was processed to yield relatively high-surface area active carbon (AC). Thirdly, the resulting carbon was employed to reversibly adsorb chromate ions from water, aiming to establish a water purification process with reusable AC. The technique used here enabled oil recovery together with the production of a clean solid, suitable for making AC. This process also has the advantage of low production cost.

© 2006 Elsevier Ltd. All rights reserved.

**Keywords:** Active carbon; Olive solid waste; Adsorption; Chromate

## 1. Introduction

Active carbon (AC) is useful in water purification (Asfour et al., 1985; McKay et al., 1986; Haimour, 1990; Catural et al., 1991; Guangwei et al., 1997; Rivera-Utrilla et al., 2003). Therefore, researchers are looking for new low-cost sources of AC. Using abundant agricultural solid wastes, in AC production, is unarguably welcome. Olive solid waste is a suitable source for mechanically stable AC. Olive trees are widely planted in the Mediterranean region. The average world production of olive oil is  $2.5 \times 10^6$  ton, most of which comes from the Mediterranean countries (Albuquerque et al., 2004). Even in small countries, like in Palestine, more than  $6 \times 10^4$  ha of land is planted with more than  $8 \times 10^6$  trees, giving an annual 20,000–30,000 tons of olive solid waste production (Annual Report on Forestry, 1997). Moreover, olive waste-based carbon seems to have special features such as low sulfur content, low ash content, high surface areas and uptake values (Martínez et al., 2006; Stavropoulos and Zabaniotou,

2005). For these reasons, it is desirable to develop routes for AC production to utilize the vast quantities of solid wastes produced in olive producing countries.

Olive seeds are usually crushed and disposed of after processing the olive oil. The aqueous liquid wastes produced by the oil mills are drained as sewage, and are beyond the scope of this study, while the solid waste is disposed with no careful management, and is of concern here. The solid waste typically contains 6–8% oil. When dumped, such oil reacts to yield hazardous chemicals such phenols and other aromatics (Caputo et al., 2003). In a few cases, the solid waste is re-pressed under costly high pressures to recover lower quality oil, useful in the soap industry. For many years, the solid waste has been partly used as inefficient polluting heating fuel (Cichelli and Solinas, 1984; Garcia et al., 1982; Amat et al., 1999). Research is underway to reverse the current negative human activities in such a way to recycle and use solid wastes for environmental cleanup.

Agricultural end products such as plant leaves and crushed solids have been used as adsorbents for water contaminants, (Aoyama et al., 1999, 2000; Dakiky et al., 2002; Pagnanelli et al., 2002; Caputo et al., 2003;

\*Corresponding author. Tel.: +970 599 273460; fax: +970 9 2387 982.  
E-mail address: hikmathilal@yahoo.com (H.S. Hilal).

Albuquerque et al., 2004; Garg et al., 2004; Fiol et al., 2006; Verma et al., 2006) despite their relatively low surface areas. Manufacturing highly porous AC, with high surface areas, from solid wastes is another strategy, because AC has the potential to be used in water purification and environmental cleanup, at an economic scale (Alkhamis and Kablan, 1999a; Kablan and Alkhamis, 1999). Examples of AC production from olive, palm, coconut and others (McKay et al., 1985; Ferro-Garcia et al., 1988; Gonzalez et al., 1994; LaGreage et al., 1994; Al-Khalid, 1995; Al-khalid et al., 1998; Caballero et al., 1997; Alvarez et al., 1998; Bacaoui et al., 1998; Alkhamis and Kablan, 1999b; Guo and Lua, 1999; Zhonghua and Srinivasan, 1999; Al-Asheh and Banat, 2001; Lafi, 2001; Dakiky et al., 2002), are known.

This work presents a three-fold strategy in utilizing solid olive waste, for the first time, in a preliminary lab scale study. Waste oil recovery, by safely extracting an extra 6–8% of waste, as useful oil for soap production, instead of dumping, is one target. Another objective is to produce AC with high surface area. The AC will be used to reversibly adsorb inorganic contaminants from water. Olive-based AC is intentionally chosen here for more than one reason. In addition to its abundance, it is robust, stable and it does not swell in aqueous media. Due to its hydrophobic nature, AC preferentially adsorbs organic matter and can be easily recovered from water suspensions.

## 2. Experimental

### 2.1. Chemicals

Solid olive wastes were provided by local olive mills from the Nablus area, West Bank, Palestine, during olive cultivation seasons (October–December). Fresh samples were stored in the dark at low temperatures. Solvents and common chemicals, such as  $K_2CrO_4$ , NaOH and acetic acid, were purchased from Aldrich Co.

### 2.2. Equipment

An atomic absorption spectrometer, Video 11-aalae (Instrumentation Laboratory Inc.) equipped with a built-in microprocessor and auto-calibration unit was used for routine analysis of aqueous  $CrO_4^{2-}$  ions. A Cr Visimax I Hollow Cathode Lamp (Thermo Jarrell Ash Corp.) working at 12 mA was used. Measurements were conducted at a wavelength of 440 nm. Ion concentrations were deduced using pre-constructed calibration curves.

### 2.3. Oil recovery

Oil was extracted from fresh olive waste using the Soxhlet method. Solid olive pips (180 g) were placed in a thimble. Solvent (80 mL, lead-free gasoline, ether or acetone) was refluxed over the solid waste for 10 min. The liquid solution, including recovered oil, was then taken

and distilled to isolate the recovered oil. In each distillation, the evaporated solvent was recovered in a cooled container, with percentage loss no more than 2%. To achieve highly concentrated oil solutions, used batches of solid pips were replaced with fresh batches. The fresh batches were then extracted using the same residual solvent. The procedure was repeated to up six times, giving concentrated oil, before final separation.

### 2.4. AC preparation

The clean solid remaining in the thimble was isolated, and dried at 45 °C. To prepare the AC, the solid was placed in a pre-cleaned dry clay dish and placed inside a tube furnace under nitrogen atmosphere. Heating was started from room temperature with a high ramp rate (above  $20\text{ }^\circ\text{C min}^{-1}$ ) reaching a steady temperature of 500 °C where heating continued for 20 min under nitrogen flow. Heating was then terminated and the system was cooled quickly with a water bath. The percentage yield of carbon was 88%, based on dry clean solid. No activating agents were used during AC production. The black AC was then isolated and stored away from moisture in a desiccator.

### 2.5. AC characterization

The AC was sieved using the conventional mesh technique, where different size fractions were collected. Particle size ranges are shown below. AC bulk density was  $483\text{ kg m}^{-3}$  which resembles literature values (<http://www.carbochem.com/activatedcarbon101.html#Properties>). Ash content was measured by incinerating AC samples (0.5 g each) at 800 °C in the air until constant weights were reached, according to the literature method (McKay et al., 1985). The ash content was less than 6% by mass, which is similar to or slightly higher than earlier reported values (Bautista-Toledo et al., 1994; Rivera-Utrilla et al., 2003; <http://www.carbochem.com/activatedcarbon101.html#Properties>).

AC surface area was measured experimentally using acetic acid adsorption (Glasstone and Lewis, 1983; Richard and Marilyn, 2004), assuming mono-layer coverage, according to Langmuir isotherms. Despite its lack of high accuracy, the acetic acid adsorption method was followed for two reasons: firstly, it is easy and safe and, secondly, it is economic. Due to lack of low-temperature experiments, it was not possible here to do  $N_2$  adsorption experiments at 77 K. The AC was washed with water several times, before drying in an oven at 120 °C. Seven glass bottles were pre-treated with acetic acid solution (0.5 M) for 60 min, rinsed with water and dried with compressed air before use in the adsorption experiments. This was to eliminate possible loss of acetic acid on container surfaces. Accurately weighed 1.00 g samples of AC, taken from the same particle size range, were placed into each of the seven pre-treated bottles. To each bottle was then added an acetic acid solution (100 mL), with concentrations ranging from 0.015

to 0.15 M. The stoppered, thermostated (25 °C) mixtures were then periodically shaken for 60 min to reach equilibrium. Each mixture was then filtered, and titrated with  $\text{NaOH}_{(\text{aq})}$  (0.1 M), using phenolphthalein indicator. The total number of moles of acetic acid adsorbed per gram of carbon ( $N$ ) was then measured for different acetic acid concentrations at equilibrium ( $C_e$ ). Plots of  $C_e/N$  vs.  $C_e$  were then constructed, according to the equation  $C_e/N = C_e/N_m + 1/k_L N_m$ , and the slope showed the number of acetic acid moles adsorbed per gram AC assuming a monolayer coverage ( $N_m$ ), as shown in Fig. 1. The total surface area  $\text{g}^{-1}$  AC was then calculated knowing the area for the acetic acid molecule as  $2.1 \times 10^{-19} \text{ m}^2 \text{ molecule}^{-1}$  (Richard and Marilyn, 2004).

### 2.6. Metal-ion adsorption experiments

AC was used to adsorb chromate ions from contaminated water samples. Stock aqueous solutions of  $\text{K}_2\text{CrO}_4$ , with different concentrations (50, 40, 30, 20 and  $10 \mu\text{g L}^{-1}$ ) were prepared and used for further dilution. Adsorption isotherms were then obtained by shaking chromate solution (100 mL) of known initial concentrations with AC (0.2 g). The remaining aqueous ion concentrations were then measured by atomic absorption spectrometry (auto-calibrated AAS). Aliquots were taken for analysis at different time durations, with continuous shaking, at room temperature. The pH values were controlled using buffer solutions. The effects of different parameters, such as particle size, ion concentration and pH, on uptake value, were studied.

### 2.7. Metal ion desorption experiments

Reversible adsorption experiments were conducted by studying the ability of chromate pre-treated AC to desorb the ions at different pH values. AC samples (0.20 g) were

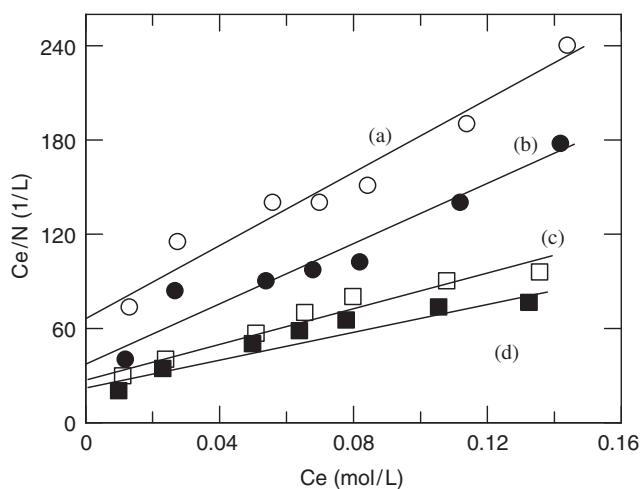


Fig. 1. Langmuir plots for acetic acid adsorption onto AC with different particle sizes: (a) 1180, (b) 850, (c) 600 and (d)  $425 \mu\text{m}$  diameters. All experiments were conducted at room temperature using 1.0 g AC.

first treated with 100 mL chromate solutions ( $120 \mu\text{g L}^{-1}$ ) at  $\text{pH} = 6$  for prolonged times (24 h) to reach equilibrium uptake ( $47 \mu\text{g g}^{-1}$  AC). The chromate pre-treated AC samples ( $\sim 0.20$  g) were then isolated, rinsed with distilled water and placed in controlled pH chromate-free solutions (100 mL) to examine desorption. The chromate pre-saturated AC was allowed to reach equilibrium with the aqueous solution for 2 h, starting with  $\text{pH} 12$ , after which the aqueous solution was analyzed for the chromate ion. The pH value was then lowered step-wise by adding dilute  $\text{HNO}_{3(\text{aq})}$  to the mixture allowing a 2 h waiting time for each step and analyzing for chromate.  $\text{HNO}_{3(\text{aq})}$  was intentionally used whereas  $\text{HCl}_{(\text{aq})}$  or  $\text{H}_2\text{SO}_{4(\text{aq})}$  were avoided, because, at lower pH values, the chromate ions form  $\text{HCrO}_4^-$  (vide infra) which in turn reacts with  $\text{HCl}_{(\text{aq})}$  to yield the chlorochromate ion  $\text{CrO}_3\text{Cl}^-$  or sulfato complex  $\text{CrO}_3(\text{OSO}_3)^{2-}$  when  $\text{H}_2\text{SO}_4$  is used (Cotton and Wilkinson, 1988). Plots of desorbed chromate concentration vs. pH were constructed as shown below.

## 3. Results and discussion

### 3.1. Oil recovery

The Soxhlet apparatus extraction technique used here is more efficient, safer and more economical than other conventional high-pressure processes. Results are encouraging. Table 1 shows that more than 5% of solid waste can possibly be recovered as oil. The resulting solid was also clean and oil free. It demanded no prolonged processing to produce AC. In fact cleaning and oil recovery occurred in a one step process, which exhibits the economic advantage of the technique. Among the different solvents used, the lead-free gasoline was the most efficient solvent.

### 3.2. AC characteristics

The average AC density for different particle sizes was measured to be  $480 \text{ kg m}^{-3}$ . The AC particle size distribution was studied using conventional sieving methods. Fig. 2 shows the mass fraction of the AC for each particle size range. SEM was also used to study the particle shapes and surface topologies together with pore structure. Fig. 3 shows a SEM micrograph for AC particles with diameters in the range  $800\text{--}1200 \mu\text{m}$ . At the macro-scale level, the particles showed different sizes with different sizes having non-spherical shapes. At the microscale level, the particles exhibited non-uniformity in pore size and shape. Inner

Table 1  
Maximum oil recovery percentage values using different solvents

	Solvent		
	Ether	Acetone	Unleaded gasoline
Maximum % oil recovery	4.4	3.7	5.4

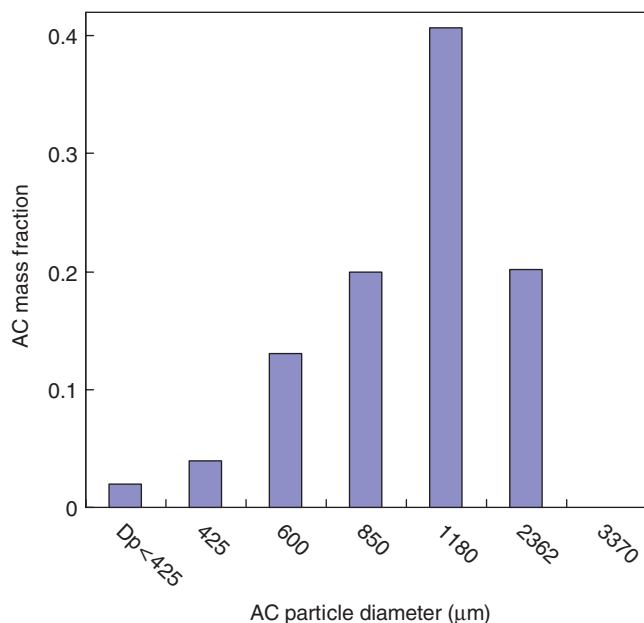


Fig. 2. AC particle size distribution showing mass fraction for each size fraction.

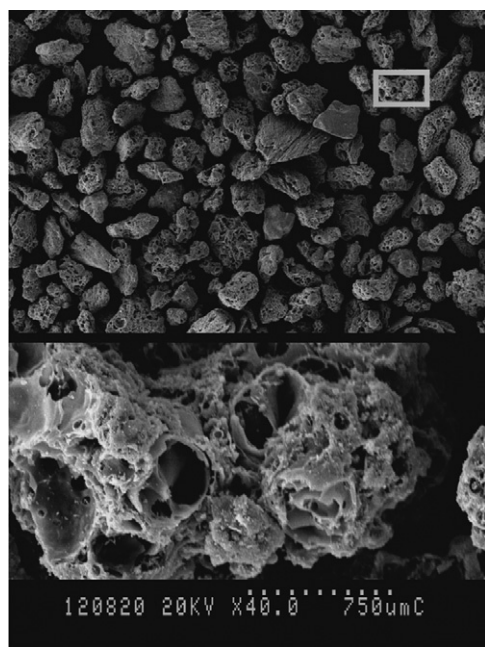


Fig. 3. SEM micrographs for AC particles, with diameters in the range 800–1200 μm.

smaller pores, within larger ones, are observed. The lack of pore size and shape uniformity is not unexpected in non-crystalline solids. Unless otherwise stated, particle sizes in the range 450–2000 μm were collected and used for adsorption and/or desorption applications.

Surface areas were measured using the adsorbed acetic acid method. The AC surface area varied for different particle sizes. The AC largest surface area ( $277 \text{ m}^2 \text{ g}^{-1}$ ) was observed for fractions of particles with sizes around

$\sim 425 \mu\text{m}$ , and the smallest ( $112 \text{ m}^2 \text{ g}^{-1}$ ) for particle sizes of  $1180 \mu\text{m}$  or larger. The observed differences in surface areas, between small and large particles, show the inefficiency of the acetic acid technique to measure the internal surface area of AC. Therefore, the measured values of the surface areas should be considered as rough approximate ones, and the actual values must be higher if micropores are taken into consideration. This has been verified by additional control experiments. The surface areas of commercial AC samples, (with known surface areas  $> 1000 \text{ m}^2 \text{ g}^{-1}$ ) were studied using the acetic adsorption method, and the measured value was  $\sim 850 \text{ m}^2 \text{ g}^{-1}$ . Despite that, the relatively high surface area of the produced AC, with no activating agents, exhibits the advantages of the process employed here. Firstly, the Soxhlet extraction system completely removes organic material from the solid surface, which provides a larger surface area in the carbon production. Moreover, it eliminates the need to add activating agents while preparing the carbon. The carbon prepared here showed relatively high surface areas, as compared to activated carbon described in earlier reports, or commercially provided, as shown in Table 2. Earlier reports (Lafi, 2001; Martínez et al., 2006; Stavropoulos and Zabaniotou, 2005) showed that olive waste has the advantage of producing carbons with especially high surface areas.

### 3.3. Chromate ion adsorption

AC samples, with different particle sizes and surface areas, were used to adsorb  $\text{CrO}_4^{2-}$  from known solutions. Equilibrium saturation was reached after 2 h of continued shaking. Adsorption isotherms are presented. Depending on the experimental conditions, relatively high adsorption uptakes were observed. Maximum adsorption uptake of chromate reached  $1.2 \text{ mg g}^{-1}$ . This value is comparable to earlier literature values observed for commercial activated carbon, where  $4.34\text{--}7.00 \text{ mg g}^{-1}$  were observed (Bautista-Toledo et al., 1994; Aoyama et al., 1999; Rivera-Utrilla et al., 2003).

#### 3.3.1. Effect of particle size

The effect of carbon particle size on chromate uptake was studied. Equilibrium chromate uptake values were measured, using different initial chromate concentrations, for each particle size fraction separately, as shown in Fig. 4.

Particle size, in the range 400–850 μm, affected the chromate uptake onto AC. Fig. 4 shows that the relative chromate uptake value, ( $\mu\text{g g}^{-1} \text{ AC}$ ) was higher for smaller particles. Such a tendency is not unexpected, as smaller particle sizes have higher relative external surface areas and, consequently, higher uptakes, as discussed earlier in Section 3.2 above.

In larger particle sizes, a different behavior was observed. Particle sizes in the range 1400–2000 μm or higher showed no significant differences in uptake values, Fig. 5 (plots b and c). In this respect, the results resemble



Table 2  
Comparison of characteristics of carbon prepared with earlier carbon

Commercial	Particle size	Surface area (m <sup>2</sup> /g)	Ash content % mass	Ref.
Olive waste based	450–2000 $\mu\text{m}$	400–120	<6	This work
Merck, catalog no. 02518	2.5 mm	1090	1.7	Rivera-Utrilla et al. (2003)
Merck (treated AC)	0.15–0.25 mm	1089	1.7	Bautista-Toledo et al. (1994)
Calgon filtrosorb 400 untreated	1 mm	1050–1200	—	Huang and Wu (1977)
Commercial activated carbons. ACF-307, ACF-310 GAC-S, GAC-E (before treatment)	—	910–1260	—	Aggarwal et al. (1999)
Super-activated carbon (from olive waste)	125–160 $\mu\text{m}$	1340–3050	—	Stavropoulos and Zabaniotou (2005)
Olive stone and walnuts	1000–3000	960	—	Martinez et al. (2006)
Filtrisorb-400	500–710 $\mu\text{m}$	1050–1200	—	McKay et al. (1985)
Acorns and olive seeds	—	1000	—	Lafi (2001)

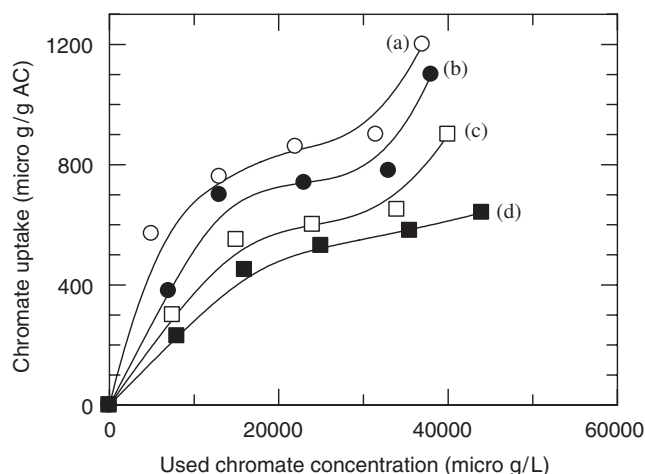


Fig. 4. Effect of AC particle size on chromate uptake: plots of equilibrium chromate uptake vs. used chromate concentration, for different AC particle sizes: (a) 425, (b) 600, (c) 850 and (d) 1180  $\mu\text{m}$ . All experiments were conducted at room temperature, using 0.2 g AC at pH 6.

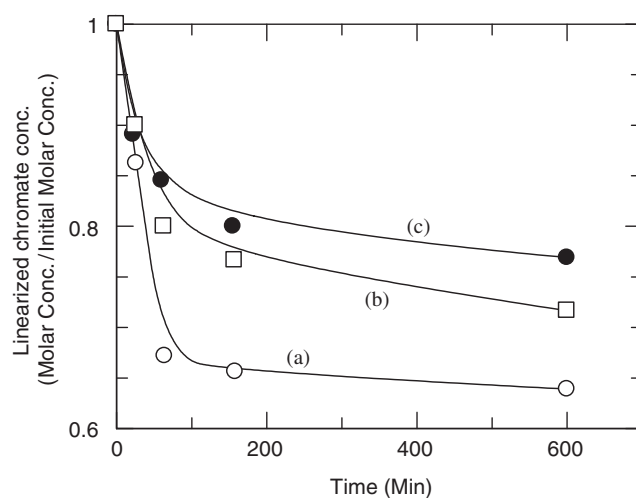


Fig. 5. Plots of linearized chromate concentration (remaining in solution) vs. time, showing chromate uptake onto AC particles with different size fractions: (a) 850, (b) 1400 and (c) 2000  $\mu\text{m}$ . All experiments were conducted at room temperature, using 0.2 g AC at pH 6.

earlier literature (Huang and Wu, 1977). On the other hand, particles larger than  $\sim 1200 \mu\text{m}$  showed uptake values lower than other smaller counterparts,  $\sim 850 \mu\text{m}$  or smaller, as shown in Fig. 5 (plots a and c).

The effect of particle size on uptake value is not explainable straightforwardly. In larger particles, particle size showed no effect, while the effect was more pronounced in smaller particles. As expected, non-crystalline AC shows low pore structure uniformity. SEM micrographs showed non-uniformity in pore structures at the micro-scale for AC with inner pores inside larger ones. The fact that larger particles, 1200  $\mu\text{m}$  or more, showed similar uptake values suggests that most of the adsorption occurs in the micropores, which are not affected by particle size. This is understandable, because as particle size increases, the relative external surface area decreases, assuming spherical shape. Therefore, the effect of external surface adsorption in such large particles

is not dominant and adsorption is attributed to micropores. In smaller particles, external surfaces become more pronounced. In these particles, both micropores and external surface affect the uptake value. This explains why smaller particles showed somewhat higher uptake.

For spherical particles, the relative external surface area (external surface area/volume) is directly proportional to  $1/\text{radius}$ . Therefore, if the external area is the dominant factor, then the uptake value should be directly proportional to  $1/\text{radius}$ . Fig. 4 shows that this is not the case. Comparison of plots (b) with (d), and (a) with (c) shows that as the particle diameter is doubled, the uptake decreases but is not halved. This is direct evidence that uptake in smaller particles external area is not the only factor that determines uptake. Internal structure and micropore adsorption are also involved, even in the smaller particles.

Langmuir and Freundlich isotherms were constructed for  $\text{CrO}_4^{2-}$  uptake experiments using different particle sizes. The Langmuir isotherms were plotted using the equation:  $C_e/Q_e = 1/k + a(C_e/k)$  and are shown in Fig. 6, where  $C_e$  is solution concentration at equilibrium ( $\mu\text{g dm}^{-3}$ );  $Q_e$  is the equilibrium  $\text{CrO}_4^{2-}$  uptake ( $\mu\text{g g}^{-1}$  AC); and  $k$  ( $\text{dm}^3 \text{g}^{-1}$ ) and  $a$  ( $\text{dm}^3 \text{mg}^{-1}$ ) are the Langmuir constants

The Freundlich isotherms were plotted using the equation  $\log(Q_e) = \log(K_f) + (1/n)\log(C_e)$  as shown in Fig. 7, where  $K_f$  is the Freundlich constant, and  $n$  is the exponential coefficient.

Langmuir and Freundlich isotherm data for chromate adsorption, onto AC with different particle sizes, are

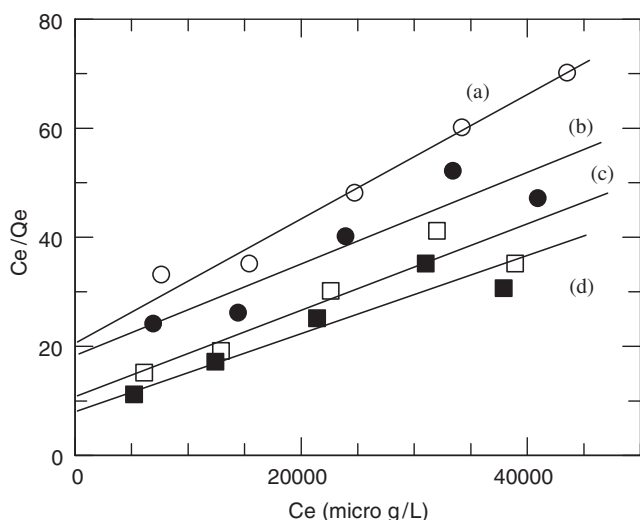


Fig. 6. Linearized Langmuir isotherms for chromate ion adsorption onto different AC particle sizes: (a) 1180, (b) 850, (c) 600 and (d) 425  $\mu\text{m}$ . All experiments were conducted at room temperature, using 0.2 g AC at pH 6.

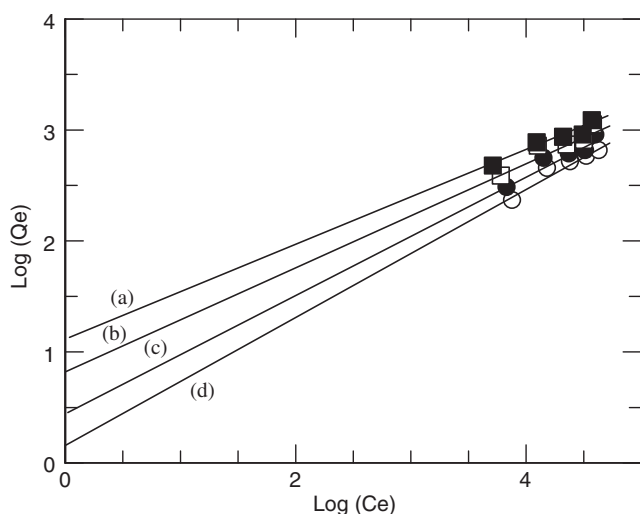


Fig. 7. Freundlich plots for chromate ion adsorption onto AC with different particle sizes: (a) 425, (b) 600, (c) 850 and (d) 1180  $\mu\text{m}$ .

summarized in Table 3. The table shows that values of  $a$ ,  $k$ , and  $k_f$  increase with decreasing particle size. The data are essential in designing batch wastewater treatment plants where the effluent concentration should be lowered from a certain value to another acceptable value using AC (McKay et al., 1985; LaGreage et al., 1994) published data on Langmuir and Freundlich constants for Filtrasorb 400 commercial AC of 500–710  $\mu\text{m}$ . The Langmuir constant value in this work is  $0.084 \text{ dm}^3 \text{ mg}^{-1}$  compared to McKay's value  $0.52 \text{ dm}^3 \text{ mg}^{-1}$ . For particles with 600  $\mu\text{m}$  diameter, the Freundlich constant and exponential coefficient values here are  $5.8 \mu\text{g g}^{-1}$  and 2.05 respectively, compared to McKay's values of  $2.3 \mu\text{g g}^{-1}$  and 0.44.

For larger particle sizes, namely 1180 and 850  $\mu\text{m}$  in diameter, the Freundlich constant and the exponential coefficient values here resemble literature values,  $2.3 \mu\text{g g}^{-1}$  and 2.27, respectively (McKay et al., 1985). The differences between the values observed here and the literature ones are not unexpected, and are possibly due to differences in the origins of the AC and particle surface topologies.

The isotherm shapes may tell if adsorption is “favorable” or “unfavorable” using the Langmuir-type adsorption process. The isotherm shape is classified by a dimensionless constant separation factor,  $r$ , where  $r = 1/(1 + aC_0)$ . Smaller values,  $r < 1$ , represent favorable adsorption, whereas larger values represent unfavorable adsorption. Values of  $r$ , measured here, are all less than 1 (ranging 0.19–0.3), as shown in Table 2, which indicates that the AC favors chromate adsorption. Such values are in agreement with McKay's.

### 3.3.2. Statistical fit

Using experimental data fitting constants, plots of  $Q_e$  vs.  $C_e$  were constructed. This procedure was followed for all results, as exemplified in Fig. 8 showing experimental plots for AC particles with 425  $\mu\text{m}$  diameter. The regression value for the curve is 0.91. (McKay et al., 1985) attributed the discrepancy, normally observed in published data, to surface area differences, and to experimental limitations. Relatively small deviations in fitting experimental results here are observed, which is presumably due to the relatively small AC surface area (only  $400 \text{ m}^2 \text{ g}^{-1}$ , compared to  $\sim 1000 \text{ m}^2 \text{ g}^{-1}$  or higher in commercial AC).

The effect of initial  $\text{CrO}_4^{2-}$  concentration on initial rate of adsorption was preliminarily studied following the method of initial rates (Bromberg, 1984). Isotherms are shown in Fig. 9. The concentration affected both the equilibrium uptake and the rate of adsorption. Within concentrations in the range  $50\text{--}200 \mu\text{g L}^{-1}$ , adsorption showed a first order dependence with respect to  $\text{CrO}_4^{2-}$ .

### 3.3.3. Effect of pH

The effect of pH on chromate ion adsorption on AC was preliminarily studied. Fig. 10 shows plots of chromate concentrations vs. time measured using different pH values. The equilibrium chromate uptake values are higher for higher pH. Furthermore, the initial rates of aqueous

Table 3  
Langmuir and Freundlich constants for different AC particle sizes

Particle diameter( $\mu\text{m}$ )	Langmuir				Freundlich		
	$a$ ( $\text{dm}^3 \text{mg}^{-1}$ )	$K$ ( $\text{dm}^3 \text{g}^{-1}$ )	$r$	$R^2$	$K_f$ ( $\text{mg g}^{-1}$ )	$n$	$R^2$
1180	$4.75 \times 10^{-2}$	0.045	0.296	0.94	1.663	1.776	0.97
850	$4.56 \times 10^{-2}$	0.056	0.305	0.92	2.679	1.852	0.85
600	$6.09 \times 10^{-2}$	0.084	0.247	0.88	5.856	2.056	0.85
425	$8.3 \times 10^{-2}$	0.117	0.194	0.93	13.6	2.405	0.91

$R^2$  indicates the least square fitting. Calculation of ( $r$ ) was based on 50 ppm initial concentration and ( $a$ ) value in Table. McKay's value was 0.23 for 500–710  $\mu\text{m}$  particles.

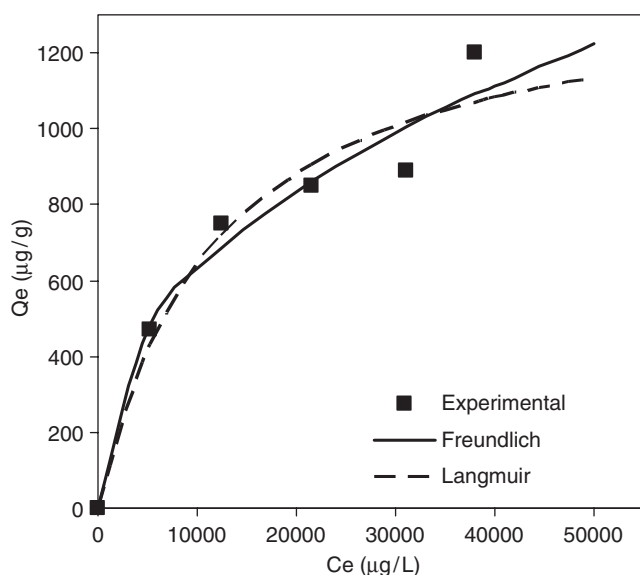


Fig. 8. Comparison of experimental data and theoretical Langmuir and Freundlich models for  $\text{CrO}_4^{2-}$  adsorbed onto AC (425  $\mu\text{m}$  in diameter), at room temperature, using pH 6.

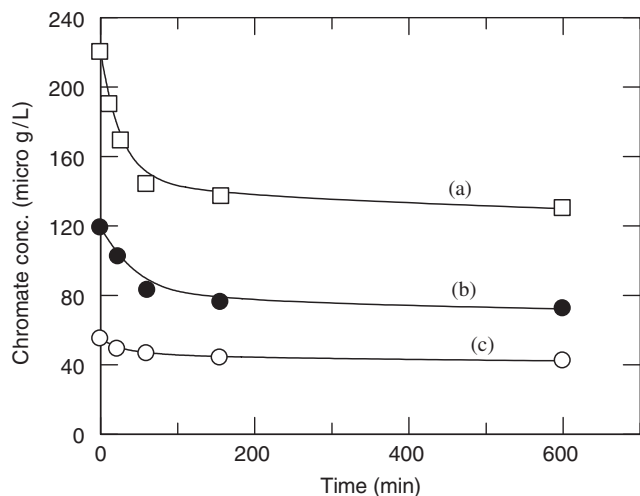


Fig. 9. Plots of remaining chromate concentration vs. time, showing effect of initial  $\text{CrO}_4^{2-}$  concentration on uptake value: (a) 220, (b) 120 and (c) 55  $\mu\text{g L}^{-1}$ . All experiments were conducted using 0.21 g AC (1400–1700  $\mu\text{m}$ ), at pH = 4.8, at room temperature. Note the especially high concentrations of Cr ions used here.

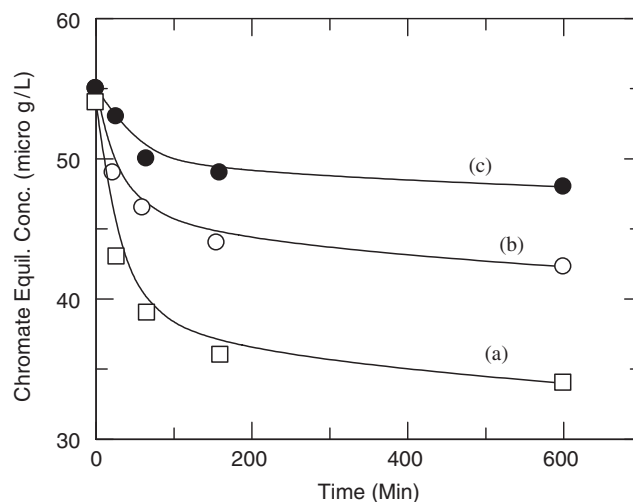


Fig. 10. Effect of pH on adsorption of  $\text{CrO}_4^{2-}$ : (a) pH 10.0, (b) pH 4.7 and (c) pH 2.0 All experiments were conducted using 0.21 g AC (1400–1700  $\mu\text{m}$  sizes), at room temperature.

chromate removal are higher at higher pH, as shown in Fig. 10.

The effect of pH on chromate ion adsorption onto different types of solids was reported in the literature. Such effect seems to be a debatable matter. Lalvani et al. (1998), reported that chromate ion adsorbs effectively onto activated carbon surfaces in the pH range 3–9, and the uptake decreases sharply at pH < 3 and pH > 9. Yu et al. (2003) showed that chromate uptake onto maple sawdust was higher at pH 6 than in more acidic media. Moreover, Aggarwal et al. (1999) showed that chromate adsorption on activated carbon increases when acidic hydrogen ions are removed from the surface. They also described the ability of highly porous activated carbon to effectively adsorb chromate negative ions in the pH range 7–10 due to the presence of positively charged sites. Furthermore, Aggarwal attributed the ability of the chromate ion to adsorb more effectively than  $\text{Cr}^{3+}$  ion, to the size differences between the two species, and concluded that adsorption is due to the activated carbon micropores. Huang and Wu (1977) showed that chromate ions adsorb onto activated carbon with maximum uptake values at pH values in the range 5–6. On the other hand, literature

showed that other adsorbents behave differently. Reports showed that chromate uptake is much higher in highly acidic media than in basic media, while using rice husk (at pH 2) (Bishnoi et al., 2004), chitosan (at pH 3) (Rojas et al., 2005), tamarind hull-waste solids (pH 1) (Verma et al., 2006), black locust leaves (pH 2) (Aoyama et al., 2000), coniferous leaves (pH 2) (Aoyama et al., 1999) and others (Dakiky et al., 2002; Garg et al., 2004; Ko et al., 2004). Based on these literature results, the following generalization could now be stated: in case of highly porous solids, such as carbon, where micropores are the dominant adsorption sites, chromate ions adsorb preferentially at higher pH values. On the other hand, in the case of solids with lower surface areas, where adsorption occurs mainly onto the external surfaces, chromate ions adsorb preferentially at lower pH values.

The carbon used in this work has a relatively large surface area, and adsorption occurs mainly in the micropores, as discussed earlier. While discussing the pH effect on uptake value, two effects associated with pH value should be considered. Firstly, the pH affects the AC surface characteristics, as at higher pH the surface becomes more of the metal ion form, and at lower pH it is more in the H-form. If chromate adsorption occurred mostly on the external solid surface, the lower pH value would enhance adsorption of the negatively charged chromate ions, by their interaction with surface acidic hydrogens. The fact that the chromate adsorption uptake value was increased at higher pH indicates that this was not the case, and that the adsorption was not facilitated by the acidic hydrogens. Secondly, the pH affects the nature of the chromate ion, as shown in Table 4. At pH values higher than 6, the ion remains in the chromate ion form  $\text{CrO}_4^{2-}$ . At pH values in the range 2–6, it exists in the form of a mixture of  $\text{HCrO}_4^-$  and  $\text{Cr}_2\text{O}_7^{2-}$  ions, and at pH values lower than 1, the ion becomes  $\text{H}_2\text{CrO}_4$  (Cotton and Wilkinson, 1988). In the presence of certain species, such as activated carbon, the Cr(III) ion is formed at lower pH values (Huang and Wu, 1977).

Therefore, as the pH is lowered, the positively charged Cr(III) ions result. When adsorption occurs at the external surfaces, the adsorption uptake of this ion must be lowered due to repulsion with the acidic AC surface in its H-form. Moreover, due to its relatively large size compared to chromate ion (Aggarwal et al., 1999), the Cr(III) may not freely enter the AC micropores. Thus at lower pH values,

Table 4  
Dominant Cr ion species distribution at different pH values (Cotton and Wilkinson, 1988; Huang and Wu, 1977)

	pH value		
	>6	2–6	<1
Dominant species	$\text{CrO}_4^{2-}$	$\text{HCrO}_4^-$ , $\text{Cr}_2\text{O}_7^{2-}$ and $\text{Cr}^{3+}$ (aq)	$\text{H}_2\text{CrO}_4$

chromium adsorption uptake is lowered. The data indicate that AC may function effectively in naturally contaminated waters, which normally have pH values around 6. Evidently, this shows the advantage of using AC in natural water purification to remove chromate. Other solids that demand highly acidic media to adsorb chromium ions may not be practical as they demand severe acidification of waters to be purified.

### 3.4. Chromium ion desorption

To investigate the potential value of AC for possible future recycle and reuse, preliminary chromate desorption from AC samples pre-treated with chromate solutions was conducted. To ensure that the adsorbed species is the chromate ion and not the Cr(III) ion, pre-treatment was conducted in non-acidic solutions. Pre-treated AC samples (uptake  $47 \mu\text{g g}^{-1}$  AC) were exposed to chromate-free aqueous solutions with different pH values, as explained in the experimental section. As the pH value was lowered, more chromium ions desorbed, Fig. 11. As explained earlier, the desorbed species of chromium ions at lower pH are not in the chromate form but presumably in the Cr(III) form. At pH values as low as 2, up to 90% of pre-adsorbed ions was desorbed and recovered back into solution within 2 h. In this respect the system is potentially useful. Aoyama et al. (2000) observed only up to 25% desorption of Cr(III), from black locust leaves, pre-treated with ions, while using 0.5 M  $\text{HNO}_3$  solutions, and up to 8% desorption while using 0.5 M NaOH solutions, after prolonged times. Such behavior indicates the occurrence of relatively strong interactions between the plant leaf surface and the pre-adsorbed chromate ions.

As the pre-adsorbed species in this work is the chromate ion, it is assumed that the desorbed species at higher pH are chromate ions, whereas at lower pH the ions should

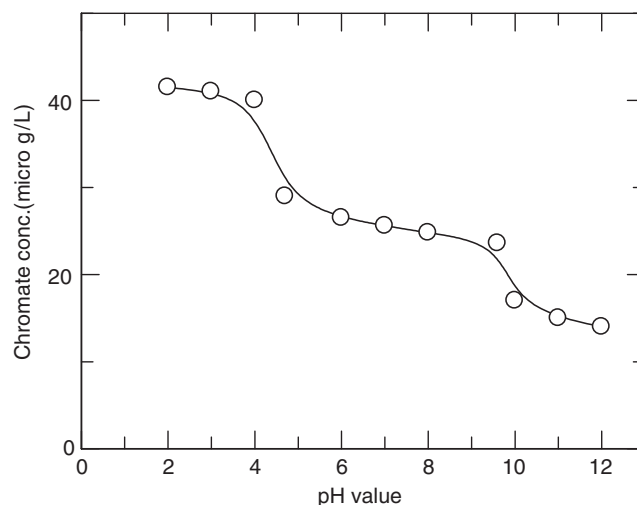


Fig. 11. Effect of pH lowering on chromate desorption from chromate pre-saturated AC. Measurements were conducted using 0.2 g pre-saturated AC, shaken with chromate-free aqueous solutions. In the desorption experiments, values of pH were lowered by adding  $\text{HNO}_3(\text{aq})$ .



include Cr(III). The fact that more desorption occurred at lower pH values is not unexpected. At lower pH the chromate/Cr(III) equilibrium is shifted towards formation of Cr(III) ions, which do not adsorb in the AC micropores as explained earlier. The desorption plot exhibited a sharp slope at pH 5, (Fig. 11). This is the pH at which the chromate ion changes to other ionic species, such as Cr(III). As the Cr(III) adsorption in the micropores is not favored, a sharp slope change in the desorption plot is expected to occur at the corresponding pH value. Desorption of other types of pre-adsorbed metal ions in a concentrated manner, from different adsorbents, has also been reported using  $\text{HNO}_{3(\text{aq})}$  and other acids (Pagnanelli et al., 2002). The high percent desorption observed here is consistent with literature (Fiol et al., 2006) where up to 85% desorption was observed.

The results indicate that a processing cycle may be established by the combined adsorption/desorption processes. The cycle simply involves two consecutive processes, contaminant adsorption at AC using higher pH values, and then contaminant desorption from the pre-saturated AC at lower pH values. The combined net outcomes of such a cycle will then be water purification and AC recovery in a clean manner. Preliminary chromate adsorption/desorption studies are encouraging more study. By this technique, AC samples may possibly be reused and the adsorbed ions may be recovered and kept under control. This shows the potential value of olive solid waste-based AC in environmental cleanup in a reusable manner. Adsorption/desorption of different types of ion pollutants, such as those of lead, copper, and other elements, onto olive solid waste-based carbon, in addition to other types of carbon will be investigated using the preparation techniques described here. Study is focused on recovering the adsorbed ions back into solutions with concentrations higher than the originally polluted samples. Pilot plant study of such a strategy is also underway to study the stability of AC after many adsorption–desorption cycles and at the end assess its feasibility at a commercial scale.

#### 4. Conclusions

A lab-scale preliminary study to utilize solid olive wastes in environmental protection has been presented. More than 5% of solid waste may be recovered as oil which may be used in soap production. The remaining solid may then be used to produce AC. The resulting AC may itself be used to adsorb inorganic contaminants from water. Recovery of both AC and contaminant ions is possible by desorption at lower pH values. A cycle processing strategy, that involves contaminant adsorption on AC at higher pH, followed by desorption at lower pH, is thus possible and needs to be further studied both at lab and pilot plant scales. The used process has the advantage of low-cost production in comparison to other commercial activated carbons used in wastewater cleaning.

#### Acknowledgments

SEM micrography service and discussions provided by Dr. Paul Sharratt and Reg Mann of the School of Chemical Engineering and Analytical Science at the University of Manchester, UK, are acknowledged. Thanks are also due to Dr. Dr Kevin Wall Research Fellow, SCEAS University of Manchester, for help in revising the manuscript. The authors wish to thank the International St. Andrews Prize 2000.

#### References

- Aggarwal, D., Goyal, M., Bansal, R.C., 1999. Adsorption of chromium by activated carbon from aqueous solution. *Carbon* 37, 1989–1997.
- Al-Asheh, S., Banat, F., 2001. Adsorption of zinc and copper Ions by the solid waste of the olive oil industry. *Adsorption Science and Technology* 19, 117–129.
- Albuquerque, J.A., Gonzalez, J., Garcia, D., Cegarra, J., 2004. Agrochemical characterisation of “alperujo”, a solid by-product of the two-phase centrifugation method for olive oil extraction. *Bioresource Technology* 91, 195–200.
- Al-Khalid, T.T., 1995. Production of activated carbon from olive expression residues (Jift) using a fluidized-bed reactor. M.Sc. Thesis, University of Jordan.
- Al-Khalid, T.T., Haimour, N.M., Sayed, S.A., Akash, B.A., 1998. Activation of olive-seed waste residue using  $\text{CO}_2$  in a fluidized-bed reactor. *Fuel Processing Technology* 57, 55–64.
- Alkhamis, T.M., Kablan, M.M., 1999a. Olive cake as an energy source and catalyst for oil shale production of energy and its impact on the environment. *Energy Conversion and Management* 40, 1863–1870.
- Alkhamis, T.M., Kablan, M.M., 1999b. A process for producing carbonaceous matter from tar sand, oil shale and olive cake. *Energy* 24, 873–880.
- Alvarez, A.G., Molina-Sabio, M., Rodriguez-Reinoso, F., 1998. An X-ray scattering investigation of the carbonization of olive stones. *Carbon* 36, 67–70.
- Amat, A.M., Arques, A., Miranda, M.A., 1999. *p*-Coumaric acid photodegradation with solar light, using a 2,4,6-triphenylpyrylium salt as photosensitizer: a comparison with other oxidation methods. *Applied Catalysis B: Environmental* 23, 205–214.
- Annual Report on Forestry, 1997. Ministry of Agriculture. Palestine.
- Aoyama, M., Sugiyama, T., Doi, S., Cho, N.-S., Kim, H.-E., 1999. Removal of hexavalent chromium from dilute aqueous solution by coniferous leaves. *Holzforchung* 53, 365–368.
- Aoyama, M., Tsuda, M., Seki, K., Doi, S., Kurimoto, Y., Tamura, Y., 2000. Adsorption of Cr(VI) from dichromate solutions onto black locust leaves. *Holzforchung* 54, 340–342.
- Asfour, H.M., Nassar, M.M., Fadali, O.A., EL-Geundi, M.S., 1985. Equilibrium studies on adsorption of basic dyes on hardwood. *Journal of Chemical Technology and Biotechnology A: Chemical Technology* 35A, 28.
- Bacaoui, A., Yaacoubi, A., Bennouna, C., Dahbi, A., Ayele, J., Mazet, M., 1998. Characterisation and utilisation of a new activated carbon obtained from Moroccan olive wastes. *Journal of Water SRT—Aqua* 47, 68–75.
- Bautista-Toledo, I., Rivera-Utrilla, J., Ferro-García, M.A., Moreno-Castilla, C., 1994. Influence of the oxygen surface complexes of activated carbons on the adsorption of chromium ions from aqueous solutions: effect of sodium chloride and humic acid. *Carbon* 32, 93–100.
- Bishnoi, N.R., Bajaj, M., Sharma, N., Gupta, A., 2004. Adsorption of Cr(VI) on activated rice husk carbon and activated alumina. *Bioresource Technology* 91, 305–307.

- Bromberg, J.P., 1984. Physical Chemistry. Allyn and Bacon, Boston, p. 891.
- Caballero, J.A., Marcilla, A., Conesa, J.A., 1997. Thermogravimetric analysis of olive stones with sulphuric acid treatment. *Journal of Analytical and Applied Pyrolysis* 44, 75–88.
- Caputo, A.C., Scacchia, F., Pelagagge, P.M., 2003. Disposal of by-products in olive oil industry: waste-to-energy solutions. *Applied Thermal Engineering* 23, 197–214.
- Catural, F., Molina-Sabio, M., Rodriguez-Reinoso, F., 1991. Preparation of activated carbon by chemical activation with  $ZnCl_2$ . *Carbon* 29, 999–1007.
- Cichelli, A.A., Solinas, M., 1984. Phenolic compounds of olive and olive oil. *Rivista Merceol* 23, 55–69.
- Cotton, F.A., Wilkinson, G., 1988. *Advanced Inorganic Chemistry*, fifth ed. Wiley, New York, p. 693.
- Dakiky, M., Khamis, M., Manassra, A., Mer'eb, M., 2002. Selective adsorption of chromium(VI) in industrial wastewater using low-cost abundantly available adsorbents. *Advances in Environmental Research* 6, 533–540.
- Ferro-Garcia, M.A., Rivera-Utrilla, J., Rodriguez-Gordillo, J., Bautista-Toledo, I., 1988. Adsorption of zinc, cadmium, and copper on activated carbons obtained from agricultural by-products. *Carbon* 26, 363–373.
- Fiol, N., Villaescusa, I., Martínez, M., Miralles, N., Poch, J., Serarols, J., 2006. Sorption of Pb(II), Ni(II), Cu(II) and Cd(II) from aqueous solution by olive stone waste. *Separation and Purification Technology* 50 (1), 132–140.
- Garcia, P.G., Quintana, M.C.D., Garrido, A., 1982. Modifications in the natural fermentation process of black olives in order to avoid spoilage. *Grasas y Aceites [GRASAS ACEITES]* 33, 9–17.
- Garg, V.K., Gupta, R., Kumar, R., Gupta, R.K., 2004. Adsorption of chromium from aqueous solution on treated sawdust. *Bioresource Technology* 92, 79–81.
- Glasstone, S., Lewis, D., 1983. *Elements of Physical Chemistry*, second ed. Macmillan Press Ltd., India, p. 566.
- Gonzalez, M.T., Molina-Sabio, M., Rodriguez-Reinoso, F., 1994. Steam activation of olive stone chars, development of porosity. *Carbon* 32, 1407–1413.
- Guangwei, W.U., Koliadima, A., Yie-Shein, H., Matijevic, E., 1997. Adsorption of dyes on nanosize modified silica particles. *Journal of Colloid Interface Science* 195, 222–228.
- Guo, J., Lua, A.C., 1999. Textural and chemical characterisations of activated carbon prepared from oil-palm stone with  $H_2SO_4$  and KOH impregnation. *Microporous Mesoporous Materials* 32, 111–117.
- Haimour, N.M., 1990. Feasibility of (Jift) for acid effluent pollution control. *Dirasat Series B* 17, 7–21.
- Huang, C.P., Wu, M.H., 1977. The removal of chromium (VI) from dilute aqueous solution by activated carbon. *Water Research* 11, 673–676.
- Kablan, M.M., Alkhamis, T.M., 1999. An experimental study for a combined system of tar sand, oil shale, and olive cake as a potential energy source in Jordan. *Biomass and Bioenergy* 17, 507–515.
- Ko, K.-R., Ryu, S.-K., Park, S.-J., 2004. Effect of ozone treatment on Cr(VI) and Cu(II) adsorption behaviors of activated carbon fibers. *Carbon* 42, 1864–1867.
- Lafi, W.K., 2001. Production of activated carbon from acorns and olive seeds. *Biomass and Bioenergy* 20, 57–62.
- LaGrege, M.D., Bingham, P.L., Evans, J.C., 1994. *Hazardous Waste Management*. McGraw Hill Inc., New York.
- Lalvani, S.B., Wiltowski, T., Hubner, A., Weston, A., Mandich, N., 1998. Removal of hexavalent chromium and metal cations by a selective and novel carbon adsorbent. *Carbon* 36, 1219–1226.
- Martinez, M.L., Torres, M.M., Guzmán, C.A., Maestri, D.M., 2006. Preparation and characteristics of activated carbon from olive stones and walnut shells. *Industrial Crops and Products* 23 (1), 23–28.
- McKay, G., Bino, M.J., Al-Tamemi, A.R., 1985. The adsorption of various pollutants from aqueous solutions on to activated carbon. *Water Research* 19, 491–495.
- McKay, G., Bino, M.J., Altemim, A., 1986. External mass transfer during the adsorption of various pollutants onto activated carbon. *Water Research* 20, 435–442.
- Pagnanelli, F., Toro, L., Veglio, F., 2002. Olive mill solid residues as heavy metal sorbent material: a preliminary study. *Waste Management* 22, 901–907.
- Retrieved on October 15, 2005 from: <http://www.carbochem.com/activatedcarbon101.html#Properties>.
- Richard, P., Marilyn, K., 2004. *Applied Colloid and Surface Chemistry*. Wiley, New York, p. 51.
- Rivera-Utrilla, J., Bautista-Toledo, I., Ferro-García, M.A., Moreno-Castilla, C., 2003. Bioadsorption of Pb(II), Cd(II), and Cr(VI) on activated carbon from aqueous solutions. *Carbon* 41, 323–330.
- Rojas, G., Silva, J., Flores, J.A., Rodriguez, A., Ly, M., Maldonado, H., 2005. Adsorption of chromium onto cross-linked chitosan. *Separation and Purification Technology* 44, 31–36.
- Stavropoulos, G.G., Zabaniotou, A.A., 2005. Production and characterization of activated carbons from olive-seed waste residue. *Microporous and Mesoporous Materials* 82, 79–85.
- Verma, A., Chakraborty, S., Basu, J.K., 2006. Adsorption study of hexavalent chromium using tamarind hull-based adsorbents. *Separation and Purification Technology*, in press.
- Yu, L.J., Shukla, S.S., Dorris, K.L., Shukla, A., Margrave, J.L., 2003. Adsorption of chromium from aqueous solutions by maple sawdust. *Journal of Hazardous Materials B* 100, 53–63.
- Zhonghua, H., Srinivasan, M.P., 1999. Preparation of high-surface-area activated carbons from coconut shell. *Microporous Mesoporous Materials* 27, 11–18.